ARMY RESEARCH LABORATORY

Strip Cell Stack Design and Mass Transfer Phenomena in a Polymer Electrolyte Membrane Fuel Cell Stack

Rongzhong Jiang and Deryn Chu

ARL-TR-2063

February 2000

The findings in this report are not to be construed as an official Department of the Army position unless so designated by other authorized documents.

Citation of manufacturer's or trade names does not constitute an official endorsement or approval of the use thereof.

Destroy this report when it is no longer needed. Do not return it to the originator.

Abstract

A type of air-breathing polymer electrolyte membrane fuel cell (PEMFC) stack with a strip design structure was investigated. Potential-current curves for this PEMFC show typical mass transfer behavior. An empirical equation was developed to describe the kinetic processes of the stack, as opposed to only a single cell. A series of experimental potential-current and power-current curves including different humidities, temperatures, and stack lengths was extremely well fitted with the equation. A concept of mass transfer impedance is defined in this report. This empirical equation can be used to calculate the mass-transfer impedance quantitatively beyond the experimental points, for example, with decreasing humidity, where the mass-transfer impedance increases considerably.

Contents

1. Introduction **1**

2. Experiment **2**

3. Results and Discussion **3**

3.1 Typical Electrochemical Behavior of Mass Transfer and Its Modeling *3*

3.2 Effect of Humidity *4*

3.3 Performance Maximization *6*

3.4 Effect of Temperature *6*

3.5 Heat Transport in Strip PEMFC Stack *8*

3.6 Effect of Stack Length *9*

3.7 Stability Test *11*

4. Conclusion **12**

Acknowledgement **12**

References **13**

Distribution **15**

Report Documentation Page **17**

Figures

1. Typical potential-current behavior of strip PEMFC stacks with mass-transfer limitation 3
2. Humidity effect on polarization behavior of strip PEMFC stacks at constant temperature of 30 °C 5
3. Mass transfer impedance versus stack current at different humidity levels 5
4. Performance of strip PEMFC stack, with and without maximization 6
5. Mass transfer impedance versus stack current, with and without maximizing stack performance 7
6. Effect of environmental temperature on strip PEMFC stack performance 7
7. Mass transfer impedance versus stack current at different environmental temperatures 8
8. Internal temperature variation with time for strip PEMFC stack at constant current operation 9
9. Comparison of strip PEMFC stack performance between short and long stacks 9
10. Mass-transfer impedance versus stack current for different lengths of stacks 10
11. Stability of strip PEMFC stack after maximization of stack performance 11

Tables

1. Electrode-kinetic and mass-transfer parameters for strip PEMFC stack at different humidity levels 5
2. Electrode-kinetic and mass-transfer parameters for strip PEMFC stack at different temperatures 8
3. Electrode-kinetic and mass-transfer parameters for different lengths of strip PEMFC stacks at maximized stack performance 10

1. Introduction

With the prominent features of light weight, low cost, high energy efficiency, high power density, nonemission, and operation at low temperature, polymer electrolyte membrane fuel cells (PEMFCs) have received much attention during the last 10 years [1–10]. Most publications concentrate on a single cell of the PEMFC or one of its components, but recently PEMFC stacks of various types and functions were developed [11–14]. The performance of a PEMFC stack is different than that of a single PEMFC cell. In this report, we explore the differences of the electrode kinetic processes between PEMFC stacks and single cells, and promote PEMFC stacks in military and civilian applications as portable power sources. An air-breathing strip PEMFC stack, one of the newest types of PEMFC stack, has two desirable aspects: First, it produces a relatively high voltage in a compact volume. Second, it uses air directly as a cathode reactant, resulting in a great decrease in weight. In the strip design, the weight per active area is about 40 percent less than that of bipolar plate stacks [15]. The air-breathing strip PEMFC stack is a two-dimensional fuel-cell stack, with individual cells in the same plane [11]. This design allows all the cells to access the same reservoir of hydrogen, and allows the opposite face to be openly exposed to the air. However, in the investigation of the strip PEMFC stack, mass-transfer phenomena were observed when the stack was operating at high current density. This is probably because of the low oxygen concentration in air [6], low humidity, or poor heat dissipation. Because it is sometimes necessary to operate at high current density, such as in an electric vehicle, understanding the electrode kinetic processes is important. Since the early 1960s, several modeling studies have been conducted that elucidate cell potential versus current density behavior [5]. However, analytic expressions for the current-potential behavior have been developed only in special cases, such as when electrode reactions are either activation and ohmic or activation and mass-transfer controlled. When all forms of over-potentials (activation, ohmic, and mass transfer) are present, as at high current density, there are no analytical solutions for the second-order differential equations. Kim et al [5] have reported mass transfer phenomena in single PEMFC cells and modeled the potential-current behaviors with an empirical equation. Our research investigates the mass-transfer behavior in the strip air-breathing PEMFC stack and analyzes the electrode kinetic processes with an empirical equation.

2. Experiment

The air-breathing PEMFC stack was composed of either 10 cells or 5 cells connected in series. The active area of each electrode is approximately 19 cm^2. The open circuit voltage was approximately 9.4 V for the 10-cell stack and 4.8 V for the 5-cell stack. The air supply to the cathode was by convection from environmental air. The H_2 fuel was supplied through a sealed compartment at the anode side, and the stack was cooled naturally. The electrolyte for the single cells was prepared with Nafion membrane (from DuPont Chemical Company). The cathode and anode both consisted of a commercially available catalyst (20% platinum on Vulcan XC-72 carbon from E-Tek) and aqueous Nafion solution. The Nafion membrane was located between the laminated cathode and anode layers, to form the membrane electrolyte assembly (MEA). The MEA was processed by hot pressing at 120 °C. The catalyst loading was 0.4 mg Pt/cm^2 for both electrodes. The MEAs, metal foams, carbon cloths, and metal meshes were held tightly to form single cells, which were linked in series to form a stack. A Matheson TF601 multimeter was used to measure the hydrogen (99.99%) flow rate. The temperature and humidity were controlled with a Tenney environmental chamber (model BTRC) and a heatless dryer (model HF 200A). A Hewlett-Packard electronic load (model 6050A) and multimeter were used to measure stack's current and voltage, respectively. The Tenney environmental chamber was controlled through a computer with Linktenn II software. In order to get reproducible results, all electrochemical measurements were taken after equilibration of temperature and humidity for 2 hr.

3. Results and Discussion

3.1 Typical Electrochemical Behavior of Mass Transfer and Its Modeling

Figure 1 shows a typical potential-current curve of a 10-cell strip air-breathing PEMFC stack. As current increases, voltage decreases, approaching 0 V. It is well known that the electrode polarization can be attributed to activation, ohmic, and mass-transfer processes. Activation occurs mainly at the beginning of the potential-current curve, the ohmic at the middle, and the mass transfer under high current conditions. Kim et al [5] and Rho et al [6] used an empirical equation to describe the potential-current behavior for a single cell. Here, we use the same equation for a PEMFC stack, but define each term differently. At low and median currents, the stack potential-current curve can be described with the following equation:

$$E_i = E_o - B \log(1000\, i) - Ri \ . \qquad (1)$$

Here, E_i (V) and i (A) are the experimentally measured stack potential and current, respectively, and E_o (V) is the open circuit potential of the stack, which is equal to the sum of open circuit potential of all single cells connected in series. B (mV dec^{-1}) is the sum of the Tafel slope for the oxygen reduction from all single cells connected in series. R (Ω) represents the sum of the resistance of all the single cells connected in series, such as resistances in the electrolyte membrane, which causes a linear variation of potential with current. The top curve in figure 1 is the computer-calculated result from equation (1), which deviates from the experimental points at higher currents.

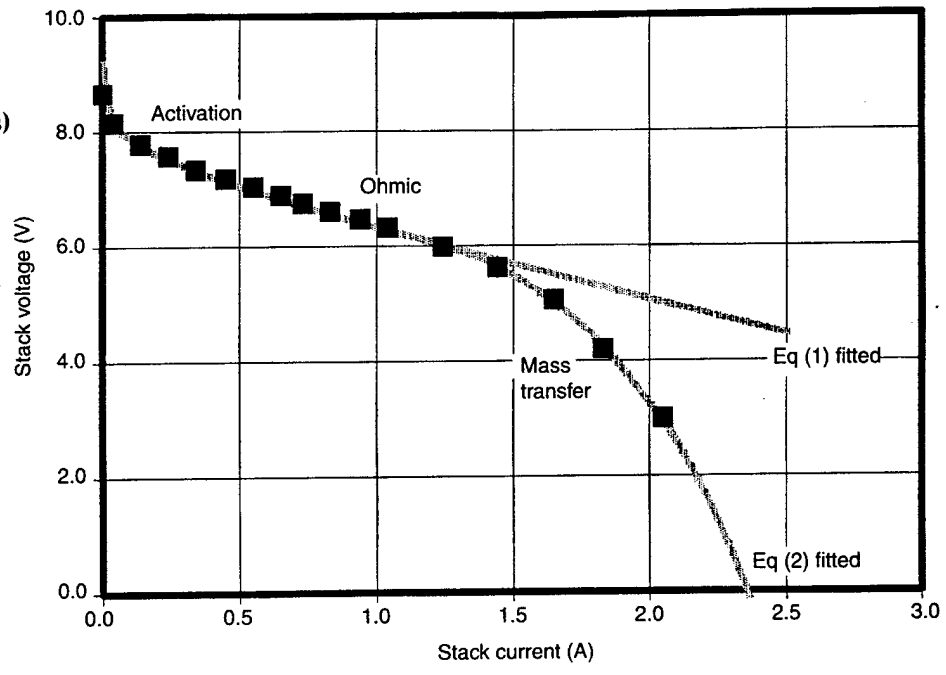

Figure 1. Typical potential-current behavior of strip PEMFC stacks (10 cells) with mass-transfer limitation. Points are obtained from experiment. Lines are computer-fitted curves with equations (1) and (2), respectively.

The entire current range of the potential-current curve can be described as

$$E_i = E_o - B \log(1000\, i) - Ri - i_m\, m \exp(n i_m) \ , \tag{2}$$

$$i_m = i - i_d \quad (\text{when } i > i_d) \ , \tag{3}$$

$$i_m = 0 \qquad (\text{when } i \le i_d) \ . \tag{4}$$

Here, i_d (A) is the smallest value of current that causes the voltage deviation from the linearity in figure 1. The i_d value can be obtained from the experimental curve or from the calculated curve with equation (1). The m (Ω) and n (A^{-1}) are the mass-transfer parameters, which can be obtained by fitting the potential-current curve with computer simulation. Equation (2) gives an excellent fit with the potential-current curves over the entire range of current. For instance, the bottom line shown in figure 1 is the computer-fitted curve with equation (2), which accurately fits the experimental points. The two lines calculated in figure 1 both give the same values of E_o, B, and R. We use equation (2) to analyze the following experimental data.

3.2 Effect of Humidity

Figure 2 shows the potential-current curves and power-current curves for the strip PEMFC stack operating at various humidity levels. The lines are fitted to the experimental points with equation (2). The voltage and power decreased with the percentage of relative humidity (RH), which implies that mass-transfer-controlled processes become more pronounced at low humidity. The power-current curves show a peak as current is increased. For RH at 90% and 70%, the maximum powers are 8.3 and 6.5 W, respectively. The kinetic parameters, obtained from computer fitting, are listed in table 1. As humidity increases, the B and R values both decrease, but the i_d value increases. The n value was kept constant during each calculation. Here we define another parameter, mass-transfer impedance (R_m), to analyze the electrode processes:

$$R_m = \Delta E / i = [i_m\, m \exp(n i_m)] / i \ . \tag{5}$$

In this study, we use only the m and n parameters to obtain the best fit with the experimental points, and we use equation (5) to calculate the mass transfer impedance beyond the range of experimental data. Figure 3 shows the calculated mass transfer impedance at 70% and 90% RH. At lower humidity, much larger mass-transfer impedance occurred. The mass-transfer impedance starts from zero and increases very quickly with current for both humidity conditions.

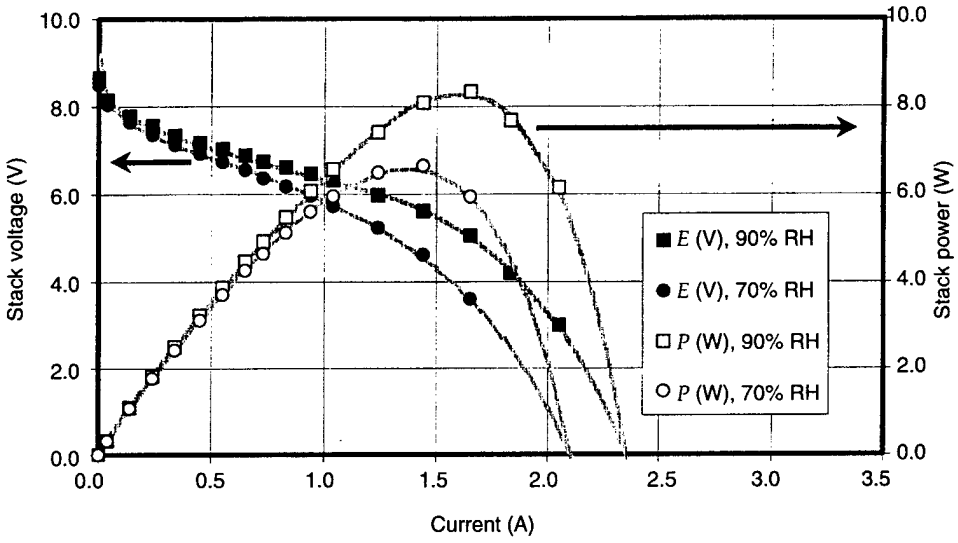

Figure 2. Humidity effect on polarization behavior of strip PEMFC stacks (10 cells) at constant temperature of 30 °C. Points and lines are experimental data and computer-fitted curves, respectively.

Table 1. Electrode-kinetic and mass-transfer parameters for strip PEMFC stack at different humidity levels. Temperature constant at 30 °C.

RH (%)	E_o (V)	B (mV dec^{-1})	R (Ω)	m (Ω)	n (A^{-1})	i_d (A)
70	9.2	680	1.1	0.36	1.5	0.65
90	9.2	600	1.08	1.0	1.5	1.34
Max.*	10.0	670	1.25	0.20	1.5	1.83

**Max. = maximized stack performance.*

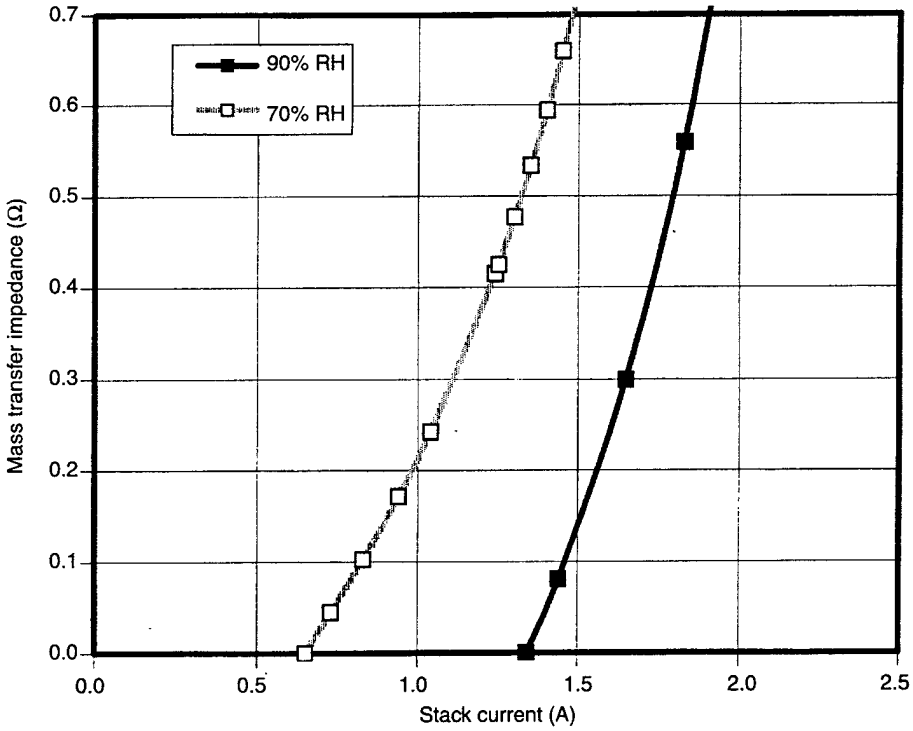

Figure 3. Mass transfer impedance versus stack current at different humidity levels. Environmental temperature is 30 °C.

3.3 Performance Maximization

The performance of the strip PEMFC was maximized under the best humidity conditions: the hydrogen gas was introduced into the stack through a gas bubbler bottle, and the stack body was covered with a wet paper towel to keep humidity at saturation. This resulted in the best performance. Figure 4 shows the potential-current and power-current curves obtained from experimental data (points) and from computer calculations (solid lines). Compared with the condition of 90% RH, the maximized curves show better performance. The peak power for the maximized condition has reached ~11 W, which is about 3 W more than at the 90% RH condition. The plot of mass transfer impedance versus stack current, with and without maximization, is shown in figure 5. The maximized curve has much smaller R_m values than that of the 90% RH condition. Initially, mass transfer impedance differs little for the two curves (only ~0.4 A current difference), but quickly becomes significant (~1.5 A current difference). The electrode kinetic parameters for the maximized condition are also shown in table 1.

3.4 Effect of Temperature

Figure 6 shows the potential-current and power-current curves for a series of environmental temperatures. At 10 °C, the potential-current curve is fitted well with equation (1), which implies that the electrode process at 10 °C is mainly controlled by activation and ohmic processes.

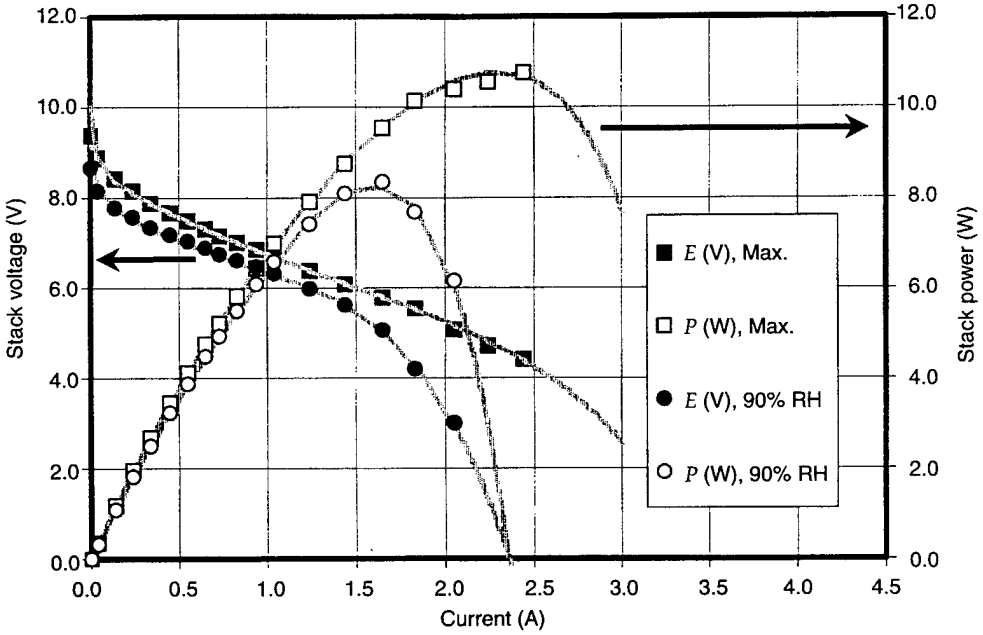

Figure 4. Performance of strip PEMFC stack (10 cells), with and without maximization. Points and lines are experimental data and computer-fitted curves, respectively.

Figure 5. Mass transfer impedance versus stack current, with and without maximizing stack performance.

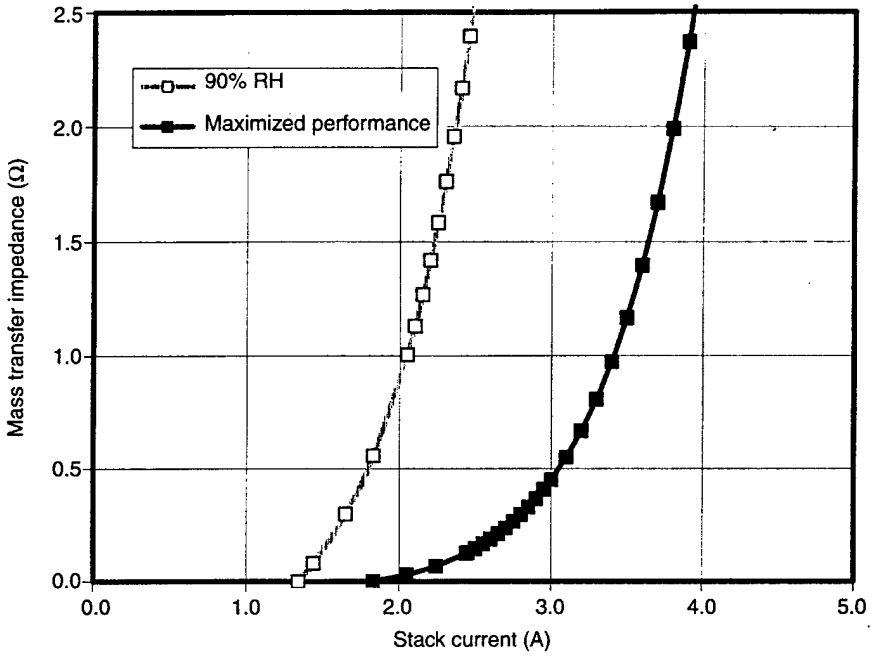

Figure 6. Effect of environmental temperature on strip PEMFC stack performance. Humidity 70% RH. Lines from top to bottom correspond to 50, 30, and 10 °C, respectively. Points and solid lines are experimental data and computer-fitted curves, respectively.

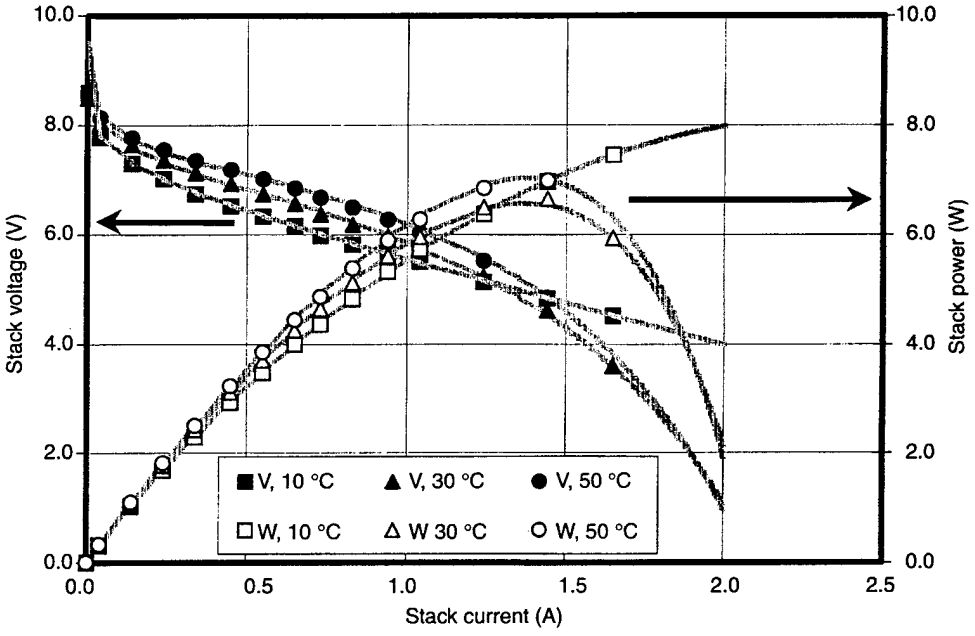

At 30 and 50 °C, equation (2) must be used to obtain the best fit with the experimental points. It is not surprising that the mass transfer impedance seems to increase with temperature. At the beginning and middle current ranges, the higher temperature provides the highest voltage and power; but at the high current range, the lower temperature delivers the highest

voltage and power. The electrode kinetic parameters obtained at different temperatures are shown in table 2. The parameters at 30 and 50 °C are only slightly different. The plot of mass transfer impedance versus stack current at temperatures 30 and 50 °C is shown in figure 7; the two curves show only slight separation (~0.1 A current difference). When the environmental temperature increases, the temperature of the internal stack will be even higher. If heat dissipation in the stack is not fast enough, the polymer electrolyte membrane and other electrode components may dehydrate, decreasing the rate of mass transfer.

3.5 Heat Transport in Strip PEMFC Stack

We inserted a thermocouple into the stack to measure its internal temperature. Figure 8 shows the internal temperature variation with time under constant current operation (1.04 A). Even when the environmental temperature is held at 30 °C, the internal temperature increases with time.

Table 2. Electrode-kinetic and mass-transfer parameters for strip PEMFC stack at different temperatures. Humidity constant at 70% RH.

T °C	E_o (V)	B (mV dec^{-1})	R (Ω)	m (Ω)	n (A^{-1})	i_d (A)
10	9.0	700	1.35	—	—	—
30	9.2	680	1.1	0.36	1.5	0.65
50	9.3	680	0.75	0.36	1.5	0.55

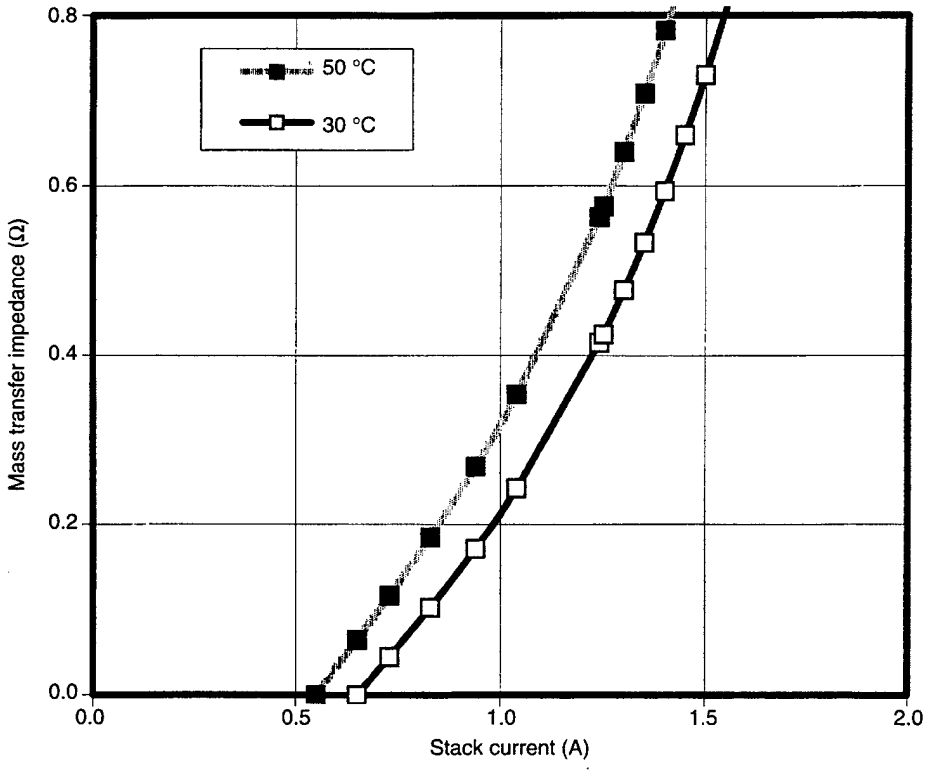

Figure 7. Mass transfer impedance versus stack current at different environmental temperatures. Humidity constant at 70% RH.

At lower humidity, the internal temperature increases faster and equilibrates slower, because of higher resistance and mass transfer impedance, which produces more heat. The slow heat transport may also limit mass transfer phenomena.

3.6 Effect of Stack Length

In order to design a high-efficiency strip PEMFC stack, we must understand the kinetic processes of different stack lengths. Figure 9 shows the

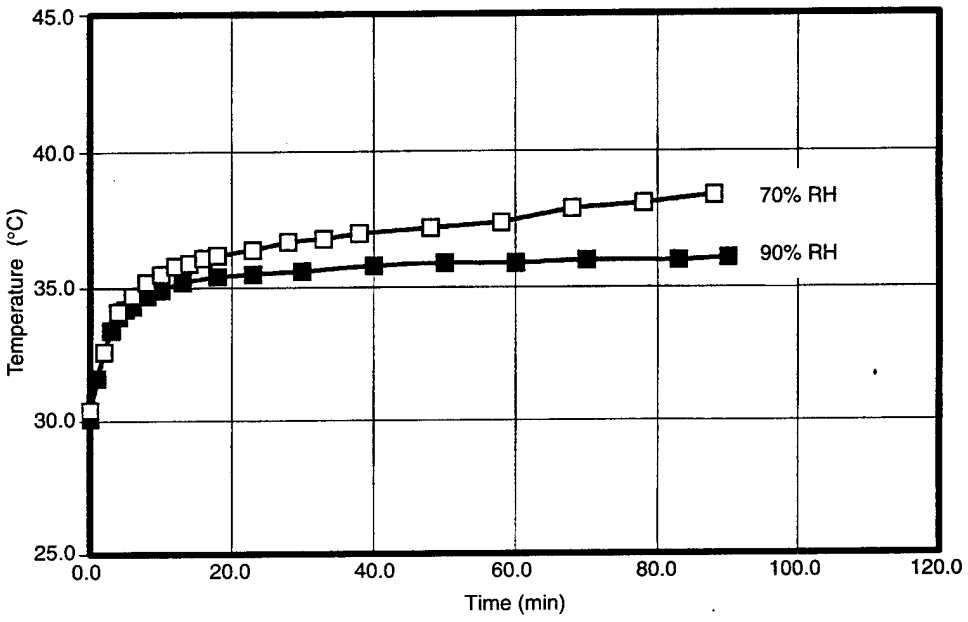

Figure 8. Internal temperature variation with time for strip PEMFC stack at constant current operation (I = 1.04 A). Environmental temperature constant at 30 °C.

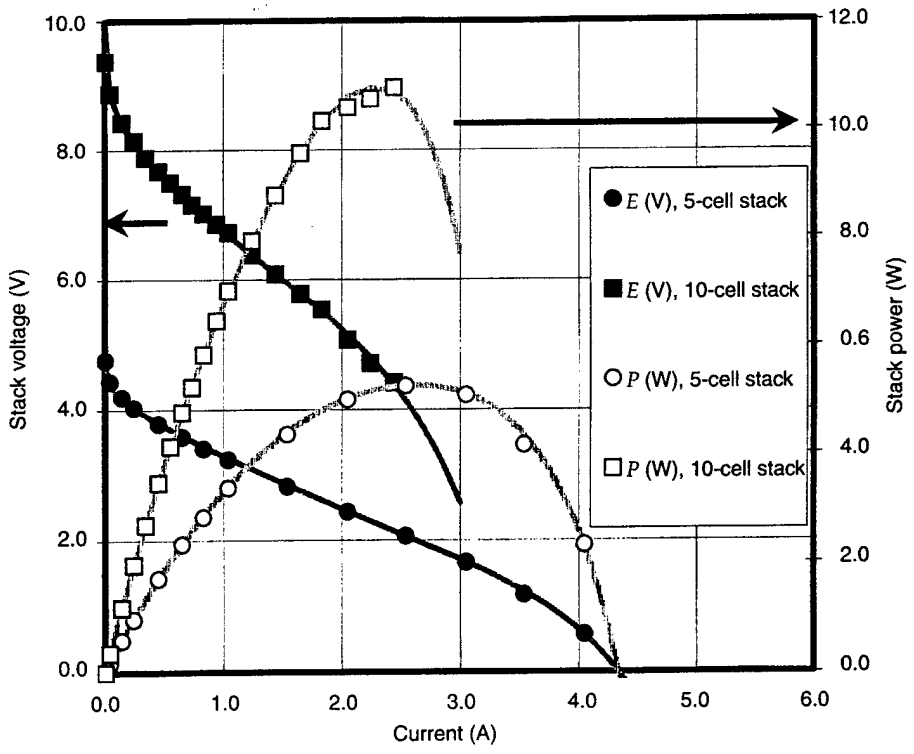

Figure 9. Comparison of strip PEMFC stack performance between short (5-cell) and long (10-cell) stacks. Performance for both stacks is maximized. Points and lines are experimental data and computer-fitted data, respectively.

potential-current and power-current curves for 5- and 10-cell stacks. The points in the figure were obtained from experimental data, and the lines were calculated with equation (2). The 5-cell stack data show much less curvature than do those of the 10-cell stack. However, the 10-cell stack has a peak power of ~11 W, while the 5-cell stack has only ~5 W. Table 3 shows the kinetic parameters obtained from the calculations. It is interesting that the parameters of E_o, B, R, and m for the 5-cell stack are about half that of the 10-cell stack, but the i_d value is about two times larger for the 5-cell stack than for the 10-cell stack. Figure 10 shows a plot of mass transfer impedance versus stack current for the 5- and 10-cell stacks. The two curves are separated by a large gap (from 1.2 to 2 A). Although the 5-cell stack has a much smaller impedance, the 10-cell stack is more efficient, because it produces a larger power density (more than double that of the 5-cell stack).

Table 3. Electrode-kinetic and mass-transfer parameters for different lengths of strip PEMFC stacks at maximized stack performance.

Length of stack	E_o (V)	B (mV dec^{-1})	R (Ω)	m (Ω)	n (A^{-1})	i_d (A)
10 cells	10.0	670	1.25	0.20	1.5	1.83
5 cells	4.95	315	0.715	0.08	1.5	3.05

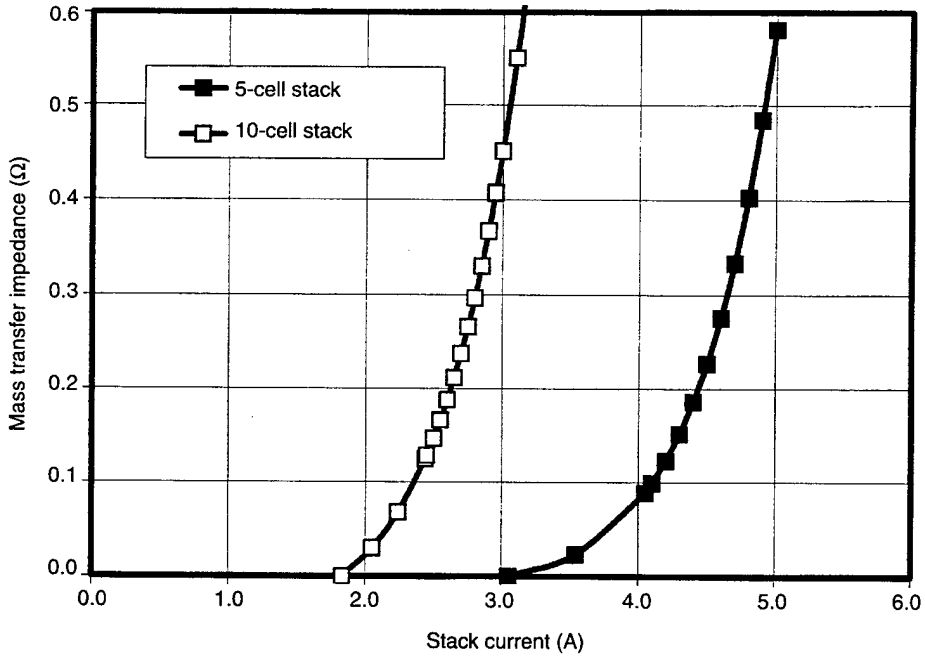

Figure 10. Mass-transfer impedance versus stack current for different lengths of stacks. Stack performance for both stacks is maximized.

3.7 Stability Test

The strip PEMFC stack was tested under constant current operation. Figure 11 shows the voltage variation with time. No voltage decrease was observed for constant current operation at 1.54 A. However, when current is increased to 2.05 A, the voltage is not stable, decreasing quickly with time—probably because of poor heat dissipation and membrane dehydration.

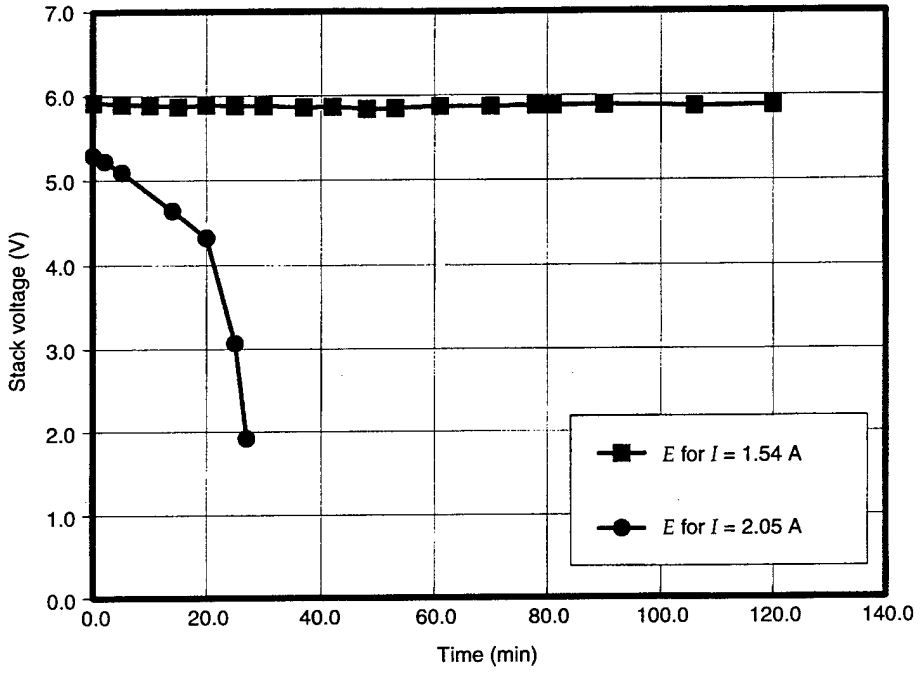

Figure 11. Stability of strip PEMFC stack after maximization of stack performance.

4. Conclusion

An empirical equation was developed to describe the electrode processes of a PEMFC stack over the entire current range, including activation, ohmic, and mass-transfer processes. The potential-current and power-current curves of the strip PEMFC stack were fitted with the empirical equation under a variety of experimental conditions, such as humidity, temperature, and stack length, and a concept of mass-transfer impedance was defined. This empirical equation can be used to calculate the mass transfer impedance beyond the experimental points. For the strip PEMFC stack, the mass-transfer impedance occurs only at high current range. With a decrease in humidity, the mass-transfer impedance increases considerably. With temperature changes from 30 to 50 °C, the mass-transfer impedance increases only slightly. For the strip PEMFC stack at low-temperature operation, less mass-transfer impedance was observed, which is attributed to a heat-transfer problem at higher environmental temperature. Increasing the total number of cells in the PEMFC strip increases the mass-transfer impedance proportionally. However, the overall power density for longer lengths of strip is larger.

Acknowledgement

The authors wish to thank the U.S. Army Materiel Command for its financial support of this project.

References

1. T. F. Fuller, *The Electrochemical Society Interface* (Fall 1997), 26.
2. E. A. Ticianelli, C. R. Derouin, and S. Srinivasan, *J. Electroanal. Chem.* **251** (1988), 175.
3. I. D. Raistrick, U.S. Patent 4,876,115 (1990).
4. M. S. Wilson and S. Gottesfeld, *J. Appl. Electrochem.* **22** (1992), 1–7.
5. J. Kim, S. M. Lee, S. Srinivasan, and C. E. Chamberlin, *J. Electrochem. Soc.* **142** (1995), 2670.
6. Y. W. Rho, O. A. Velev, S. Srinivasan, and Y. T. Kho, *J. Electrochem. Soc.* **141** (1994), 2084.
7. H. F. OetJen, V. M. Schmidt, U. Stimming, and F. Trila, *J. Electrochem. Soc.* **143** (1996), 3838.
8. M. Uchida, Y. Aoyama, N. Eda, and A. Ohta, *J. Electrochem. Soc.* **142** (1995), 4143.
9. F. N. Buchi, B. Gupta, O. Haas, and G. G. Scherer, *J. Electrochem. Soc.* **142** (1995), 3044.
10. M. Uchida, Y. Aoyama, N. Eda, and A. Ohta, *J. Electrochem. Soc.* **142** (1995), 463.
11. J. B. Lakeman and J. Cruickshank, *Proc. 38th Power Sources Conference*, Cherry Hill, NJ (June 1998), p 420.
12. A. C. Oliver and E. Clarke, *Proc. 38th Power Sources Conference*, Cherry Hill, NJ (June 1998), p 424.
13. L. P. Jarvice and D. Chu, *Proc. 38th Power Sources Conference*, Cherry Hill, NJ (June 1998), p 428.
14. O. Polevaya and D. Bloomfield, *Proc. 38th Power Sources Conference*, Cherry Hill, NJ (June 1998), p 416.
15. C. E. Chamberlin, P. A. Lehman, R. M. Reid and T. G. Herron, in *Hydrogen Energy Process X*, D. Block and T. N. Veziroglu, eds., Proc. 10th World Hydrogen Energy Conference **3**, International Association for Hydrogen Energy, Cocoa Beach, FL (20–24 June 1994), pp 1659–1663.

Distribution

Admnstr
Defns Techl Info Ctr
Attn DTIC-OCP
8725 John J Kingman Rd Ste 0944
FT Belvoir VA 22060-6218

Ofc of the Secy of Defns
Attn ODDRE (R&AT)
The Pentagon
Washington DC 20301-3080

OSD
Attn OUSD(A&T)/ODDR&E(R) R J Trew
Washington DC 20301-7100

AMCOM MRDEC
Attn AMSMI-RD W C McCorkle
Redstone Arsenal AL 35898-5240

CECOM
Attn PM GPS COL S Young
FT Monmouth NJ 07703

CECOM Night Vsn/Elect Sensors Directrt
Attn AMSEL-RD-NV-D
FT Belvoir VA 22060-5806

Commander
CECOM R&D
Attn AMSEL-IM-BM-I-L-R Stinfo Ofc
Attn AMSEL-IM-BM-I-L-R Techl Lib
Attn AMSEL-IM-BM-I-L R Hamlen
FT Monmouth NJ 07703-5703

Deputy for Sci & Techlgy
Attn Ofc Asst Sec Army (R&D)
Washington DC 30210

AF Wright Aeronautical Labs
Attn R Marsh
AFWAL-POOS-2
Wright-Patterson AFB, OH 45433

Dir for MANPRINT
Ofc of the Deputy Chief of Staff for Prsnnl
Attn J Hiller
The Pentagon Rm 2C733
Washington DC 20301-0300

Hdqtrs
Attn DAMA-ARZ-D F D Verderame
Washington DC 20310

US Army ARDEC
Attn AMSTA-AR-TD M Fisette
Bldg 1
Picatinny Arsenal NJ 07806-5000

Commander
US Army CECOM
Attn AMSEL-RD-CZ-PS-B M Brundage
FT Monmouth NJ 07703-5000

US Army CECOM Rsrch Dev & Engrg Ctr
Attn AMSEL-RD-AS-BE E Plichta
FT Monmouth NJ 07703-5703

US Army Edgewood RDEC
Attn SCBRD-TD G Resnick
Aberdeen Proving Ground MD 21010-5423

US Army Info Sys Engrg Cmnd
Attn ASQB-OTD F Jenia
FT Huachuca AZ 85613-5300

US Army Natick RDEC Acting Techl Dir
Attn SSCNC-T P Brandler
Natick MA 01760-5002

US Army Simulation, Train, & Instrmntn Cmnd
Attn J Stahl
12350 Research Parkway
Orlando FL 32826-3726

US Army Tank-Automtv Cmnd Rsrch, Dev, & Engrg Ctr
Attn AMSTA-TA J Chapin
Warren MI 48397-5000

US Army Train & Doctrine Cmnd
Battle Lab Integration & Techl Directrt
Attn ATCD-B J A Klevecz
FT Monroe VA 23651-5850

Distribution (cont'd)

US Military Academy
Mathematical Sci Ctr of Excellence
Attn MDN-A LTC M D Phillips
Dept of Mathematical Sci Thayer Hall
West Point NY 10996-1786

Nav Rsrch Lab
Attn Code 2627
Washington DC 20375-5000

Nav Surface Warfare Ctr
Attn Code B07 J Pennella
17320 Dahlgren Rd Bldg 1470 Rm 1101
Dahlgren VA 22448-5100

Marine Corps Liaison Ofc
Attn AMSEL-LN-MC
FT Monmouth NJ 07703-5033

USAF Rome Lab Tech
Attn Corridor W Ste 262 RL SUL
26 Electr Pkwy Bldg 106
Griffiss AFB NY 13441-4514

DARPA
Attn S Welby
3701 N Fairfax Dr
Arlington VA 22203-1714

Hicks & Associates Inc
Attn G Singley III
1710 Goodrich Dr Ste 1300
McLean VA 22102

Palisades Inst for Rsrch Svc Inc
Attn E Carr
Attn Documents
1745 Jefferson Davis Hwy Ste 500
Arlington VA 22202-3402

US Army Rsrch Ofc
Attn AMSRL-RO-D C Chang
Attn AMSRL-RO-EN B Mann
PO Box 12211
Research Triangle Park NC 27709-2211

US Army Rsrch Lab
Attn AMSRL-CI-AS Mail & Records Mgmt
Attn AMSRL-CI-AT Techl Pub (3 copies)
Attn AMSRL-CI-LL Techl Lib (3 copies)
Attn AMSRL-D R W Whalen
Attn AMSRL-DD J Miller
Attn AMSRL-RO-PS R Paur
Attn AMSRL-SE J Pelligrino
Attn AMSRL-SE-D E Scannell
Attn AMSRL-SE-DC D Chu (25 copies)
Attn AMSRL-SE-DC S Gilman
Attn AMSRL-SE-DC R. Jiang
Attn AMSRL-SE-E J Mait
Attn AMSRL-SS
Adelphi MD 20783-1197

REPORT DOCUMENTATION PAGE

Form Approved
OMB No. 0704-0188

1. AGENCY USE ONLY *(Leave blank)*	2. REPORT DATE	3. REPORT TYPE AND DATES COVERED
	February 2000	Progress, 10/98–9/99

4. TITLE AND SUBTITLE Strip Cell Stack Design and Mass Transfer Phenomena in a Polymer Electrolyte Membrane Fuel Cell Stack

5. FUNDING NUMBERS
DA PR: —
PE: 62120A

6. AUTHOR(S) Rongzhong Jiang and Deryn Chu

7. PERFORMING ORGANIZATION NAME(S) AND ADDRESS(ES)
U.S. Army Research Laboratory
Attn: AMSRL-SE-DC email: dchu@arl.mil
2800 Powder Mill Road
Adelphi, MD 20783-1197

8. PERFORMING ORGANIZATION REPORT NUMBER
ARL-TR-2063

9. SPONSORING/MONITORING AGENCY NAME(S) AND ADDRESS(ES)
U.S. Army Research Laboratory
2800 Powder Mill Road
Adelphi, MD 20783-1197

10. SPONSORING/MONITORING AGENCY REPORT NUMBER

11. SUPPLEMENTARY NOTES
ARL PR: 9NV4VV
AMS code: 622120.H16

12a. DISTRIBUTION/AVAILABILITY STATEMENT Approved for public release; distribution unlimited.

12b. DISTRIBUTION CODE

13. ABSTRACT *(Maximum 200 words)*

A type of air-breathing polymer electrolyte membrane fuel cell (PEMFC) stack with a strip design structure was investigated. Potential-current curves for this PEMFC show typical mass transfer behavior. An empirical equation was developed to describe the kinetic processes of the stack, as opposed to only a single cell. A series of experimental potential-current and power-current curves including different humidities, temperatures, and stack lengths was extremely well fitted with the equation. A concept of mass transfer impedance is defined in this report. This empirical equation can be used to calculate the mass-transfer impedance quantitatively beyond the experimental points, for example, with decreasing humidity, where the mass-transfer impedance increases considerably.

14. SUBJECT TERMS
Strip cell, fuel cell

15. NUMBER OF PAGES
22

16. PRICE CODE

17. SECURITY CLASSIFICATION OF REPORT	18. SECURITY CLASSIFICATION OF THIS PAGE	19. SECURITY CLASSIFICATION OF ABSTRACT	20. LIMITATION OF ABSTRACT
Unclassified	Unclassified	Unclassified	UL

NSN 7540-01-280-5500

Standard Form 298 (Rev. 2-89)
Prescribed by ANSI Std. Z39-18
298-102